Non-thermal emission from high-energy binaries through interferometric radio observations

Benito Marcote Martín

PhD Thesis

Advisors: Marc Ribó & Josep M. Paredes

U B Universitat de Barcelona

Departament d'Astronomia i Meteorologia

ICCUB Institut de Ciències del Cosmos

October 27, 2015

Outline of the PhD Thesis

Introduction

- The γ-ray sky
- Binary systems with γ-ray emission
- Motivation of this Thesis

Part I: Gamma-ray binaries

- LS 5039 and its low-frequency emission (GMRT, VLA, WSRT)
- LS I +61 303 and its low-frequency emission (GMRT and LOFAR)
- HESS J0632+057, new EVN observations

Part II: Colliding wind binaries

- HD 93129A, a new colliding wind binary discovered

Part III: Searching for new possible gamma-ray binaries

- The candidate TYC 4051-1277-1
- MWC 656, the first Be/BH binary system

Summary and conclusions

Introduction

The gamma-ray sky

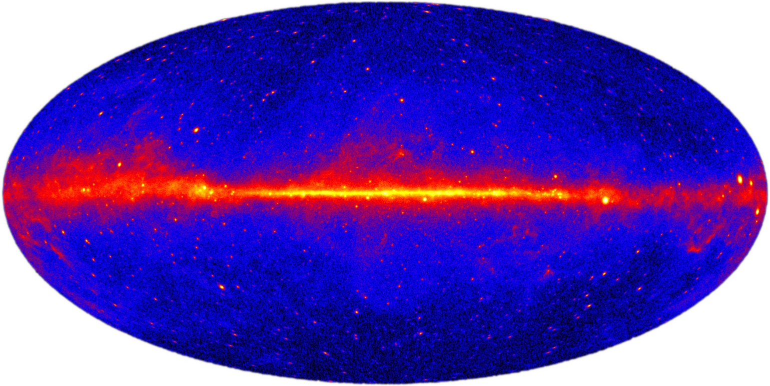

All-sky map obtained with the Large Area Telescope (LAT) detector on board the *Fermi* satellite above 1 GeV. NASA/DOE/*Fermi*/LAT Collaboration

$\sim 3\,000$ sources are known to emit at these energies

Introduction

The gamma-ray sky

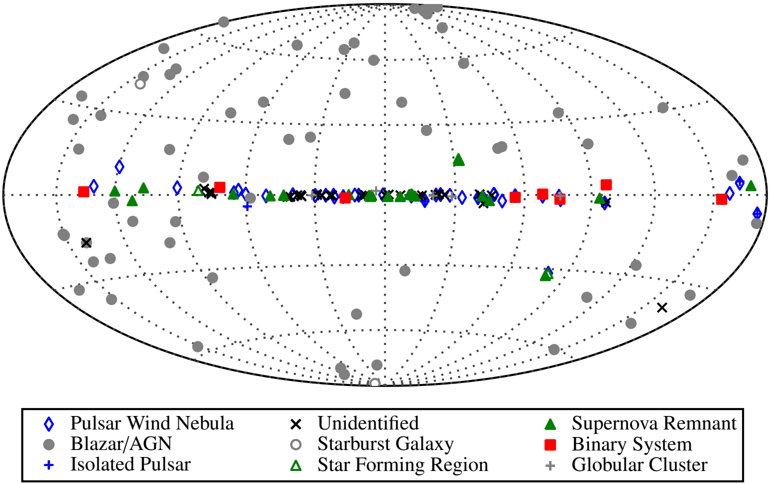

Very high-energy γ-ray all-sky map showing the 161 sources discovered up to now emitting at TeV energies. TevCat catalog (`tevcat.uchicago.edu`)

Introduction

Binary systems with γ-ray emission

γ-ray emitting sources associated to (Galactic) binary systems, usually displaying non-thermal emission from radio to γ-rays

All these binaries are composed of, at least, one **massive early-type star**, with spectral types O or early B:

$$M \sim 10 \text{ to } \sim 150\ \mathrm{M}_\odot, \quad v_\infty \sim 10^3\ \mathrm{km\ s^{-1}}, \quad T_{\rm eff} \sim 20\,000\text{–}50\,000\ \mathrm{K}$$

Three different types, as a function of the companion and the nature of the emission:

- Colliding wind binaries
- High-mass X-ray binaries
- Gamma-ray binaries

Introduction

Binary systems with γ-ray emission

System type	radio emission	γ-ray emission	Powering source
Colliding wind binaries (CWBs)	Sync	IC	wind collision
High-mass X-ray binaries (HMXBs)	Sync	IC	accretion/ejection
Gamma-ray binaries	Sync	IC?	wind collision?

Sync: synchrotron emission from radio to X-rays by a population of accelerated electrons
IC: Inverse Compton scattering of stellar UV photons by the same population of electrons

...but big differences emerge from the details.

Introduction

Colliding Wind Binaries (CWBs)

Two massive stars with powerful stellar winds
Colliding winds that produce a strong shock observed at radio, X-rays and sometimes gamma-rays

Only one CWB detected at γ-rays: η **Carina**, the most massive CWB system known:

$\sim$90–120 $\mathrm{M}_\odot$	Luminous Blue Variable star
$\sim$30 $\mathrm{M}_\odot$	O star

$P_\mathrm{orb} \sim 5.5$ yr
$e \sim 0.9$
Separation at periastron: 1.7 AU

(Tavani et al. 2009, Abdo et al. 2009, Reitberger et al. 2015, Damineli et al. 2008, Teodoro et al. 2012)

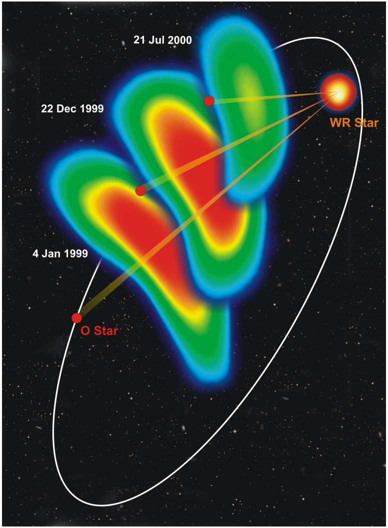

WR 140 and its wind collision region observed at radio frequencies (Dougherty et al. 2005)

Introduction

High-Mass X-Ray Binaries (HMXBs)

Massive star and compact object (NS or BH)
Spectral Energy Distribution (SED) dominated by thermal X-ray emission due to the presence of an accretion disk around the compact object

Only three HMXBs detected at γ-rays:

System	Main star	$P/$ days
Cygnus X-3	WR	0.2
Cygnus X-1	O9.7 Ve	5.6
MWC 656	Be	60.4

For these systems the γ-ray emission only appears occasionally

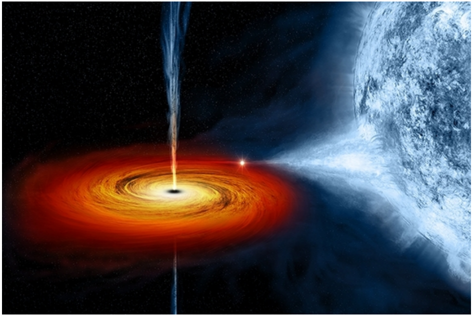

Chandra X-Ray Observatory, NASA

Some HE binaries with a compact object exhibit a different behavior:

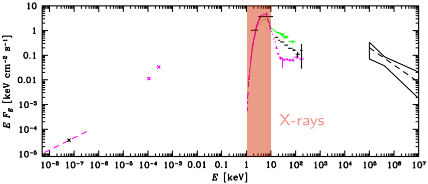

The HMXB Cygnus X-3
(Zdziarski et al. 2012)

LS I +61 303
(Sidoli et al. 2006)

Some HE binaries with a compact object exhibit a different behavior:

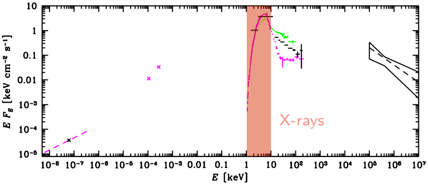

The HMXB Cygnus X-3
(Zdziarski et al. 2012)

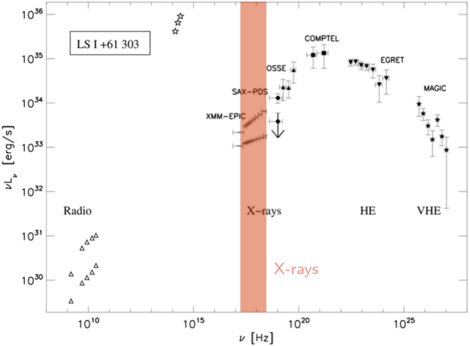

LS I +61 303
(Sidoli et al. 2006)

Introduction

Gamma-Ray Binaries

Massive star and compact object (NS or BH)
Non-thermal SED dominated by the γ-ray emission probably produced by the presence of shocks between the non-relativistic stellar wind and the relativistic wind from the compact object

The whole population of gamma-ray binaries consists currently of five systems:

System	Main star	$P/$ days
LS 5039	O6.5 V	3.9
1FGL J1018.6–5856	O6 V	16.6
LS I +61 303	B0 Ve	26.5
HESS J0632+057	B0 Vpe	315.0
PSR B1259–63	O9.5 Ve	1236.7

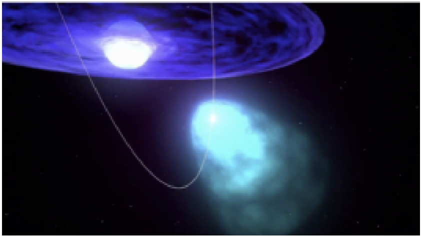

Representation of PSR B1259–63
NASA

Motivation of this Thesis

- HE binaries are good laboratories that accelerate particles up to relativistic energies, connecting particle physics to astrophysics
- γ-ray emission produced by IC from the same electron population that generates the emission from radio to X-rays by synchrotron
- Radio observations emerge thus as a powerful tool to study in detail physical properties of the emitting regions in these HE systems
- In particular, the low frequencies remain unexplored and can provide important clues about the absorption processes and their physical parameters
- VLBI observations can resolve the radio emission and distinguish the different regions that produce the emission

The aim of this thesis is thus to improve our knowledge about the emitting regions of high-energy binary systems through radio observations

Motivation and overview

Low and high-frequency interferometric observations

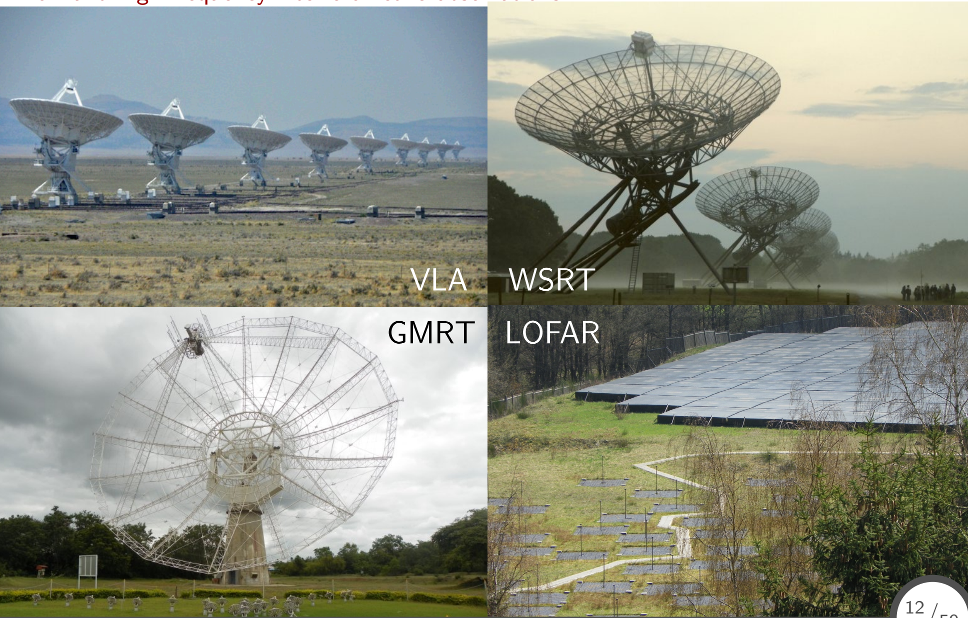

Motivation and overview

Very Long Baseline Interferometric (VLBI) observations

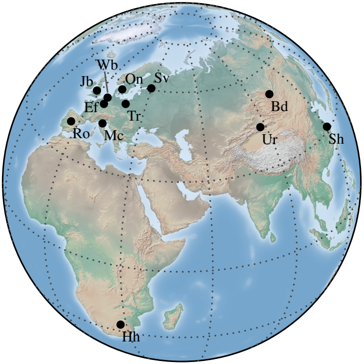

The European VLBI Network (EVN)

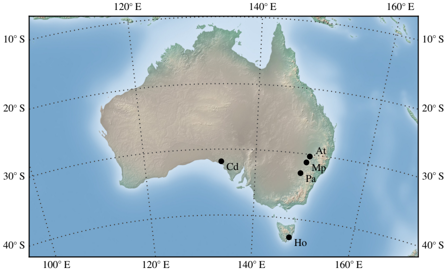

The Australian Long Baseline Array (LBA)

Outline of the PhD Thesis

Introduction
- The γ-ray sky
- Binary systems with γ-ray emission
- Motivation of this Thesis

Part I: Gamma-ray binaries
- LS 5039 and its low-frequency emission (GMRT, VLA, WSRT)
- LS I +61 303 and its low-frequency emission (GMRT and LOFAR)
- HESS J0632+057, new EVN observations

Part II: Colliding wind binaries
- HD 93129A, a new colliding wind binary discovered

Part III: Searching for new possible gamma-ray binaries
- The candidate TYC 4051-1277-1
- MWC 656, the first Be/BH binary system

Summary and conclusions

Gamma-Ray Binaries

Young non-accreting pulsar scenario

Strong shock between both winds:

- Relativistic pair plasma wind from the pulsar
- Non-relativistic stellar wind from the massive companion star

leads to particle acceleration

Originally proposed by Maraschi & Treves (1981), re-proposed by Dubus (2006)

- **Radio flux** produced by synchrotron processes (Bosch-Ramon 2009)
- **High energy** emission produced by synchrotron (X rays) and IC (γ-rays)

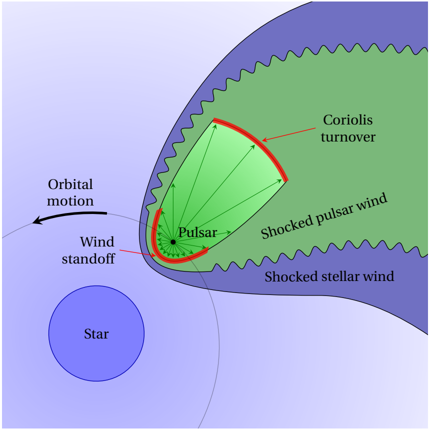

Model for LS 5039 (Zabalza et al. 2012)

The gamma-ray binary LS 5039

LS 5039

$$\alpha_{\mathrm{J2000}} = \ \ 18^{\mathrm{h}}\ 26^{\mathrm{m}}\ 15.06^{\mathrm{s}}$$
$$\delta_{\mathrm{J2000}} = -14^{\circ}\ 50'\ 54.3''$$

O6.5 V star ($23 \pm 3\ \mathrm{M}_{\odot}$)
Compact object, NS or BH (1–5 $\mathrm{M}_{\odot}$)

$P \approx 3.9$ d
$e = 0.35 \pm 0.04$
$d = 2.5 \pm 0.5$ kpc

X-rays: periodic
GeV light-curve: periodic (anticorrelated)
TeV light-curve: periodic
Radio: persistent, small variability without orbital modulation

Aharonian et al. (2005), Casares et al. (2005), Kishishita et al. (2009), Abdo et al. (2009), Casares et al. (2012), Zabalza et al. (2013), Collmar & Zhang (2014)

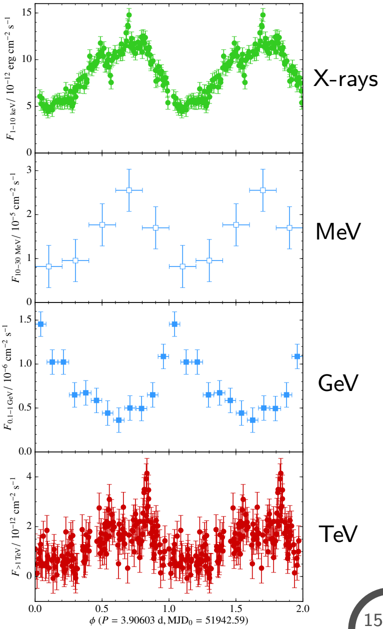

The gamma-ray binary LS 5039

LS 5039

$$\alpha_{\rm J2000} = \quad 18^{\rm h}\ 26^{\rm m}\ 15.06^{\rm s}$$
$$\delta_{\rm J2000} = -14^\circ\ 50'\ 54.3''$$

O6.5 V star ($23 \pm 3\ \mathrm{M}_\odot$)
Compact object, NS or BH (1–$5\ \mathrm{M}_\odot$)

$P \approx 3.9$ d
$e = 0.35 \pm 0.04$
$d = 2.5 \pm 0.5$ kpc

X-rays: periodic
GeV light-curve: periodic (anticorrelated)
TeV light-curve: periodic
Radio: persistent, small variability without orbital modulation

Aharonian et al. (2005), Casares et al. (2005), Kishishita et al. (2009), Abdo et al. (2009), Casares et al. (2012), Zabalza et al. (2013), Collmar & Zhang (2014)

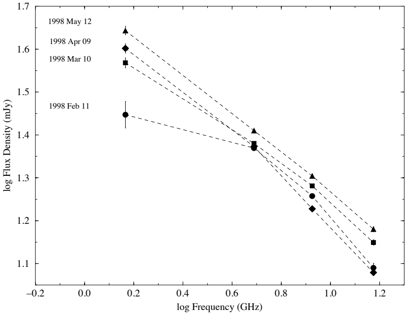

Radio spectra from 1.4 to 15 GHz

Spectral index $\alpha = -0.46 \pm 0.01$, where $S_\nu \propto \nu^\alpha$

Variability $< \pm 25$ %.

Martí et al. (1998)

Previous radio observations of LS 5039

The radio emission is resolved at VLBI scales (Moldón et al. 2012)

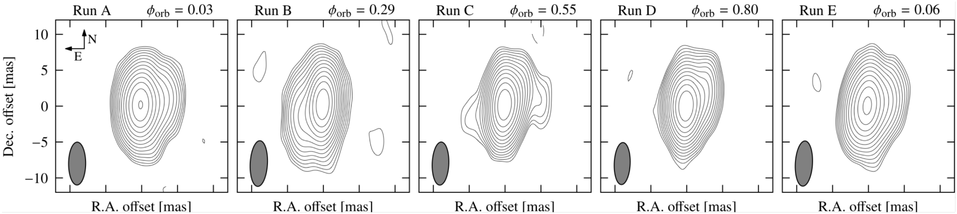

Observations along one orbital period

Dominant core emission ($\lesssim$ 1 mas, or 3 AU)

Extended emission orbitally modulated at mas scales (<10% of the total flux density)

Previous radio observations of LS 5039

At low frequencies, only a few observations have been published with contradictory results.

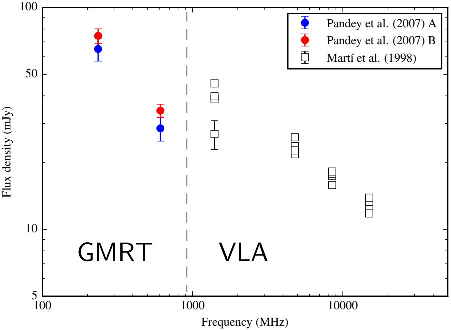

Adapted from Pandey et al. (2007)

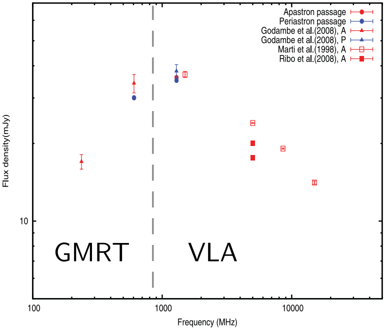

Bhattacharyya et al. (2012)
Godambe et al. (2008)

Important differences in the calibration procedures

Summary of the observations analyzed in this work

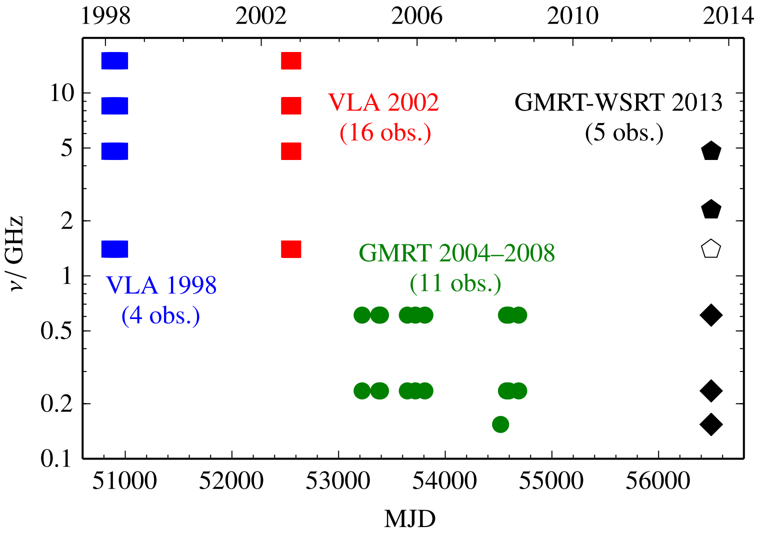

VLA and GMRT archival observations analyzed in this work
GMRT-WSRT observations proposed and analyzed as PI in 2013

Summary of the observations analyzed in this work

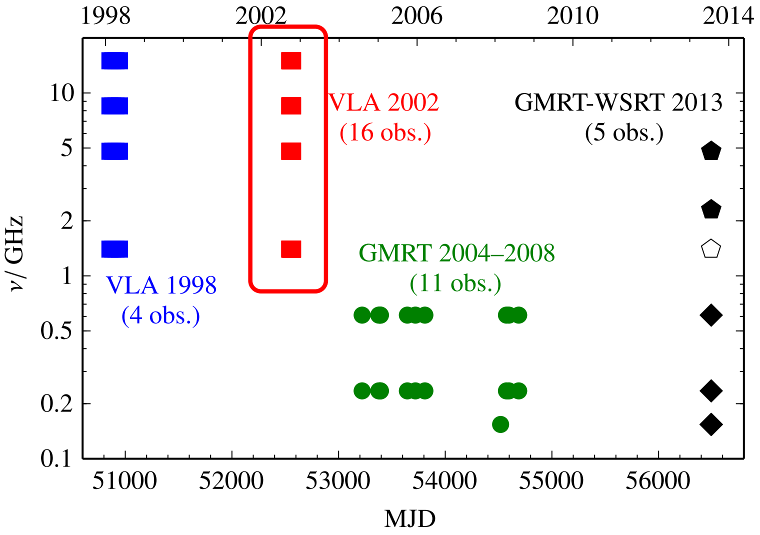

VLA and GMRT archival observations analyzed in this work
GMRT-WSRT observations proposed and analyzed as PI in 2013

High-frequency variability

VLA monitoring in 2002

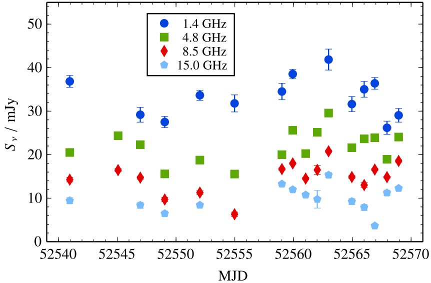

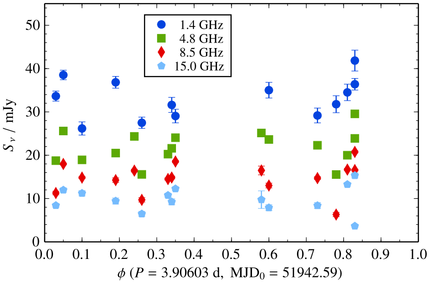

- Persistent flux density emission
- Variability on timescales as short as one day

- Variability $< \pm 25$ %
- No visible orbital modulation

Flux density values compatible with the ones reported at other epochs (e.g. Martí et al. 1998)

High-frequency variability

VLA monitoring in 2002

- Dashed lines: power-laws determined from 5.0 and 8.5 GHz
- $\approx$ power-law at GHz frequencies
- Slight curvature < 2 GHz
- Average spectral index: $\alpha = -0.57 \pm 0.12$

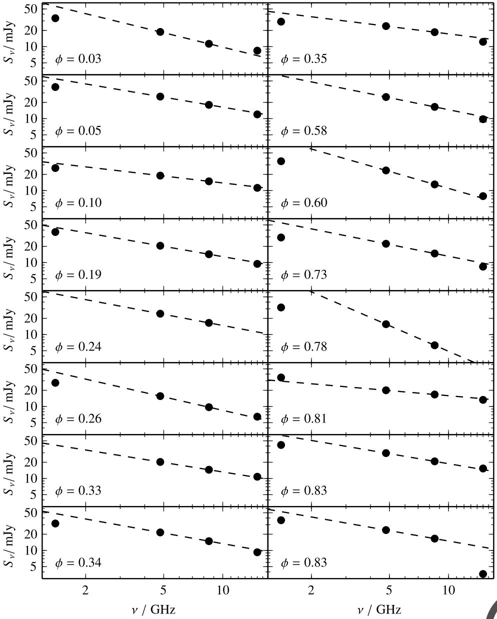

Low-frequency variability

Archival GMRT observations 2004–2008

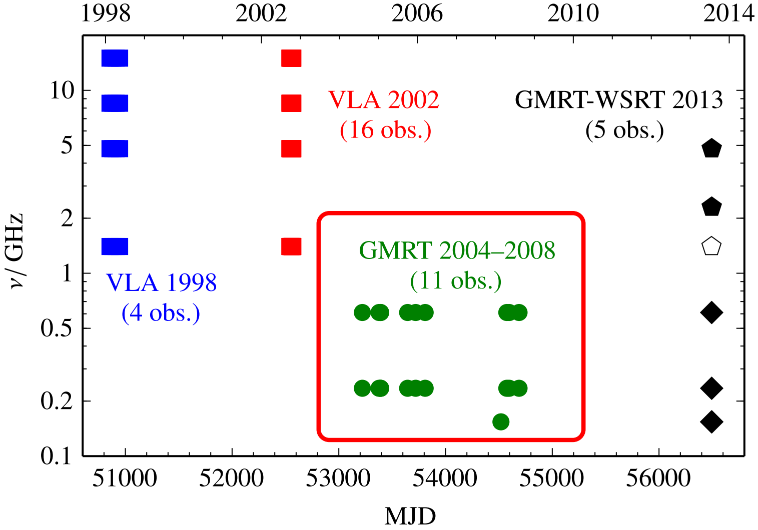

VLA and GMRT archival observations analyzed in this work

GMRT-WSRT observations proposed and analyzed as PI in 2013

Low-frequency variability

Archival GMRT observations 2004–2008

- Observations spread over 4 yr
- Persistent emission
- Variability at $> 6\sigma$
- No orbital modulation
- Average spectral index $\alpha = +0.5 \pm 0.8$

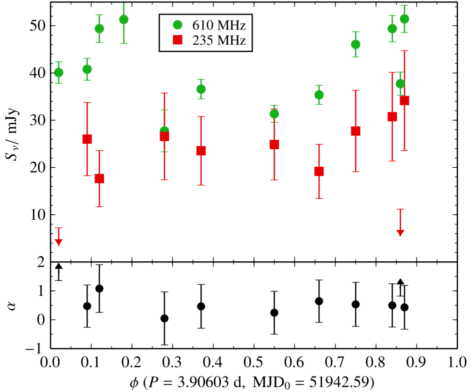

Non-simultaneous spectrum of LS 5039

Combining data from 1998 to 2013

- Small variability along the years ($< 25\,\% \quad \forall\ \nu$)
- "Similar" profile in average
- Turnover at ~ 0.5 GHz
- Source undetected at 150 MHz

- Only two data points at 2.3 GHz (not representative)
- The mean square errors have been used in the average data

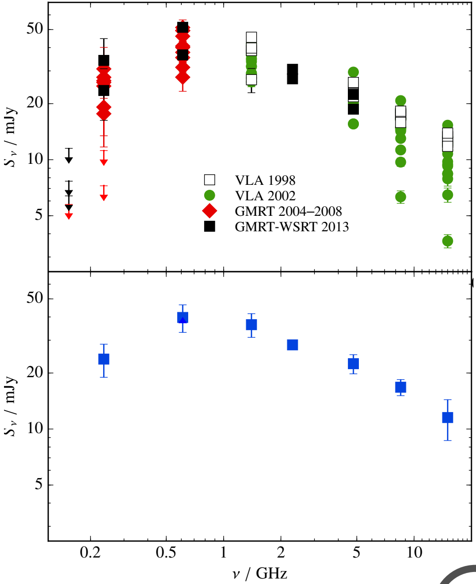

Modeling the LS 5039 spectrum

A first approximation (toy model)

Most of the radio emission comes from a compact core $\lesssim 1$ mas or ~ 3 AU (semi major axis: 0.19 AU) (Moldón et al. 2012)

We have built a very simple model to understand the spectrum:

- Compact core $\rightsquigarrow$ one-zone model
- No orbital modulation $\rightsquigarrow$ symmetric emitting region (spheric)
- For simplicity $\rightsquigarrow$ isotropic and homogeneous
- We consider the presence of a synchrotron emitting plasma
- Turnover produced by either SSA, FFA or Razin effect (and combinations of them)

Modeling the LS 5039 spectrum

A first approximation (toy model)

We have built a very simple model to understand the spectrum:

- **Synchrotron emission**, with a particle injection:

$$n(E)\mathrm{d}E = KE^{-p}\mathrm{d}E$$

- **Synchrotron self-absorption** (SSA), from relativistic plasma:

$$\kappa_{\mathrm{SSA}} \propto KB^{(p+2)/2}\nu^{-(p+4)/2}$$

- **Free-free absorption** (FFA), from thermal plasma:

$$\kappa_{\mathrm{FFA}} \propto n_{\mathrm{e}}^2 T_{\mathrm{w}}^{-3/2}\nu^{-2}$$

- **Razin effect**, from thermal plasma:

$$S_\nu \rightsquigarrow S_\nu e^{-\nu_{\mathrm{R}}/\nu}, \qquad \nu_{\mathrm{R}} \equiv 20 n_{\mathrm{e}} B^{-1}$$

Non-simultaneous spectrum of LS 5039

Combining data from 1998 to 2013

- The average spectrum can be fitted by typical models:
  - SSA
  - Synchrotron + FFA
  - SSA + Razin
  - FFA + Razin
  - SSA + FFA
- Small differences between fits
- SSA+Razin is the best fit
- But the other fits are not statistically rejected

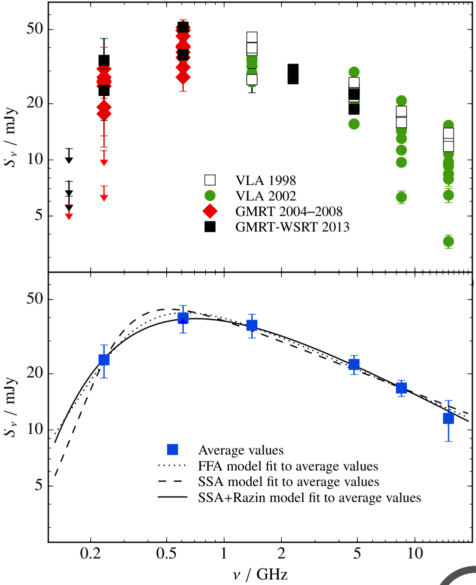

Quasi-simultaneous spectrum of LS 5039

GMRT & WSRT campaign in 2013 July 19 and 21

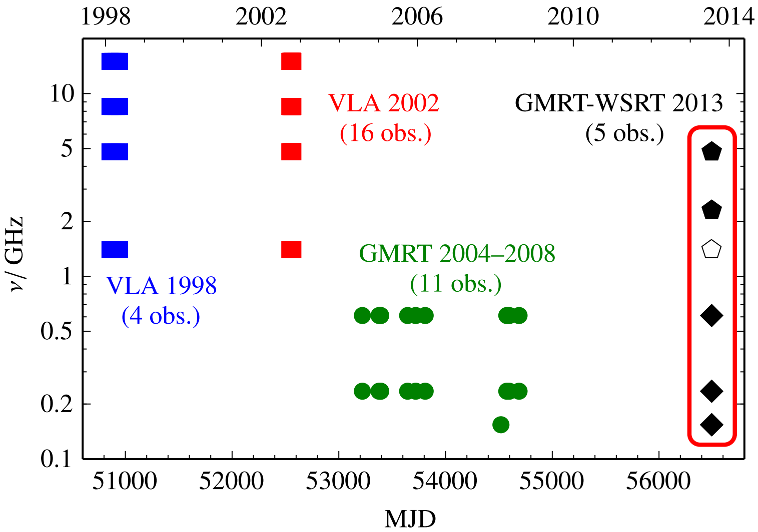

VLA and GMRT archival observations analyzed in this work

GMRT-WSRT observations proposed and analyzed as PI in 2013

Quasi-simultaneous spectrum of LS 5039

GMRT & WSRT campaign in 2013 July 19 and 21

Two 0.15–5 GHz spectra at orbital phases $\phi \approx 0.9$ and 0.4

- Similar spectra, but subtle differences between the two epochs
- Persistent turnover at ~ 0.5 GHz
- Stronger emission on 2013 July 19
- 2013 July 19: pure SSA spec.
- 2013 July 21: SSA+Razin spec.
- FFA provides poor fits

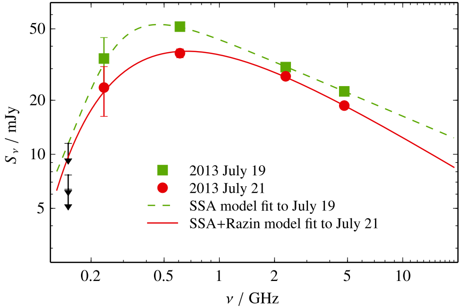

GMRT data: 235 and 610 MHz
WSRT data: 2.3 and 5.0 GHz

154 MHz GMRT data taken every other day (on 2013 July 18, 20 and 22)

Modeling the LS 5039 spectrum

The three spectra show a similar shape but with subtle differences:

- Avg. spectrum: SSA+Razin
- July 19 spectrum: SSA
- July 21 spectrum: SSA+Razin

Fit	p	$\Omega B^{-1/2}$ $\left[10^{-16}\,\mathrm{G}^{-1/2}\right]$	$K\ell B^{(p+2)/2}$ $\left[10^{3}\,\mathrm{cm\,G}^{(p+2)/2}\right]$	ν_{R} $\left[10^{8}\,\mathrm{Hz}\right]$
Avg. spectrum	2.16 ± 0.04	500 ± 800	3 ± 5	4.1 ± 0.2
July 19	1.867 ± 0.014	3.9 ± 0.3	$(2.1 \pm 0.9) \times 10^{6}$	–
July 21	2.24 ± 0.08	200 ± 600	0.4 ± 1.7	4.1 ± 0.7

- Estimating the free-free opacity from the stellar wind:

$$\tau_{\nu}^{\mathrm{FF}} \propto \dot{M}\,\nu^{-2}\ell^{-3}v_{\mathrm{w}}^{-2}T_{\mathrm{w}}^{-3/2}$$

Modeling the LS 5039 spectrum

Coherent picture from fits and τ_ν^{FF}

- Avg. spectrum: SSA+Razin
- July 19 spectrum: SSA
- July 21 spectrum: SSA+Razin

- Coherent picture with:

$$\ell \sim 0.85 \text{ mas } (\sim 2.5 \text{ AU})$$
$$B \sim 20 \text{ mG}$$
$$n_e \sim 4 \times 10^5 \text{ cm}^{-3}$$
$$\dot{M} \sim 5 \times 10^{-8} \text{ M}_\odot \text{ yr}^{-1}$$

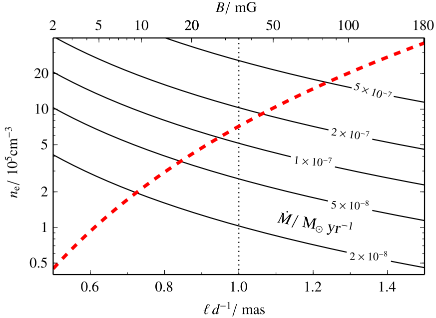

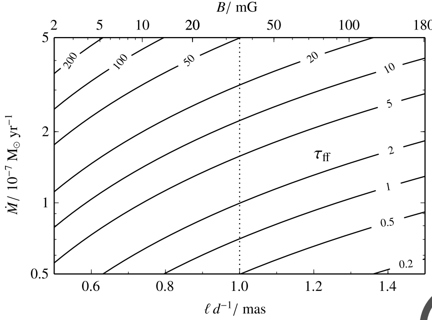

Modeling the LS 5039 spectrum

Coherent picture from fits and τ_ν^{FF}

- Avg. spectrum: SSA+Razin
- July 19 spectrum: SSA
- July 21 spectrum: SSA+Razin

- Coherent picture with:

$$\ell \sim 0.85 \text{ mas } (\sim 2.5 \text{ AU})$$
$$B \sim 20 \text{ mG}$$
$$n_e \sim 4\times10^5 \text{ cm}^{-3}$$
$$\dot{M} \sim 5\times10^{-8}\ \mathrm{M_\odot\ yr^{-1}}$$

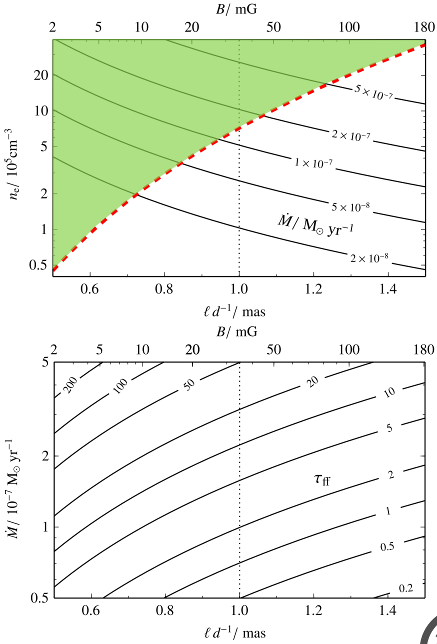

Modeling the LS 5039 spectrum

Coherent picture from fits and τ_ν^{FF}

- Avg. spectrum: SSA+Razin
- July 19 spectrum: SSA
- July 21 spectrum: SSA+Razin

- Coherent picture with:

$$\begin{aligned} \ell &\sim 0.85\ \mathrm{mas}\ (\sim 2.5\ \mathrm{AU}) \\ B &\sim 20\ \mathrm{mG} \\ n_{\mathrm{e}} &\sim 4\times10^{5}\ \mathrm{cm}^{-3} \\ \dot{M} &\sim 5\times10^{-8}\ \mathrm{M_\odot\ yr^{-1}} \end{aligned}$$

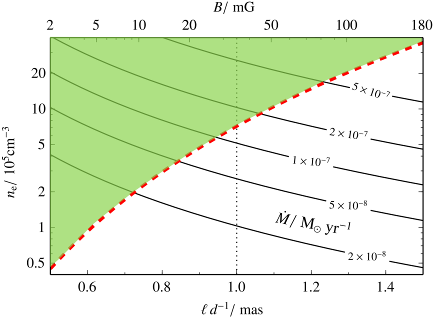

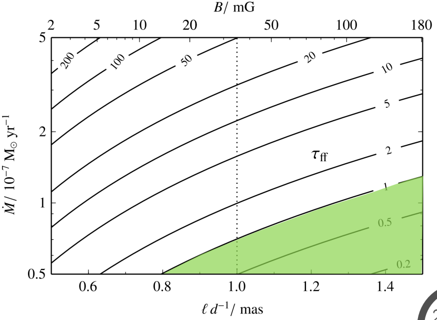

Modeling the LS 5039 spectrum

Coherent picture from fits and τ_ν^{FF}

- Avg. spectrum: SSA+Razin
- July 19 spectrum: SSA
- July 21 spectrum: SSA+Razin

- Coherent picture with:

$$\ell \sim 0.85 \text{ mas } (\sim 2.5 \text{ AU})$$
$$B \sim 20 \text{ mG}$$
$$n_{\mathrm{e}} \sim 4 \times 10^5 \text{ cm}^{-3}$$
$$\dot{M} \sim 5 \times 10^{-8} \text{ M}_\odot \text{ yr}^{-1}$$

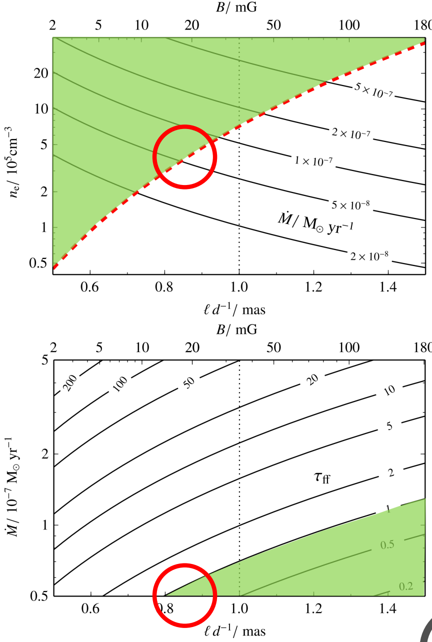

Conclusions from the modeling

- **Significant mixing** of the non-relativistic wind inside the synchrotron radio emitting relativistic plasma, even close to $\sim 100\%$ (consistent with recent simulations, e.g. Bosch-Ramon et al. 2012,2015)

- The derived mass-loss rate (model dependent, but in agreement with recent results from Casares et al., in prep.) implies that the **wind is clumpy**

- Presence of **Razin effect**, widely observed in Colliding Wind Binaries, that gives further support to the scenario of the **young non-accreting pulsar**

Conclusions

RESULTS

- We report day to day variability, trends on week timescales, and the absence of orbital variability. Variability $< \pm 25$ % is observed at all frequencies (0.23–15 GHz) even on year timescales
- Persistent turnover at around ~ 0.5 GHz
- Upper-limits for the emission at 150 MHz

DISCUSSION

- A simple model explains the observed spectra, indicating that the turnover is dominated by SSA
- Razin effect is observed at some epochs
- We have obtained a coherent picture that explains the observed spectra

FUTURE

- More accurate data (specially at low frequencies) will allow us to work with more detailed models and understand the geometry of the radio emitting region

Outline of the PhD Thesis

Introduction

- The γ-ray sky
- Binary systems with γ-ray emission
- Motivation of this Thesis

Part I: Gamma-ray binaries

- LS 5039 and its low-frequency emission (GMRT, VLA, WSRT)
- LS I +61 303 and its low-frequency emission (GMRT and LOFAR)
- HESS J0632+057, new EVN observations

Part II: Colliding wind binaries

- HD 93129A, a new colliding wind binary discovered

Part III: Searching for new possible gamma-ray binaries

- The candidate TYC 4051-1277-1
- MWC 656, the first Be/BH binary system

Summary and conclusions

The gamma-ray binary LS I +61 303

LS I +61 303

B0 Ve star ($12.5 \pm 2.5\ \mathrm{M}_\odot$)
$d = 2.0 \pm 0.2$ kpc
$e = 0.72 \pm 0.15$

$P_{\rm orb} = 26.496 \pm 0.003$ d
$P_{\rm super} = 1667 \pm 8$ d

Variability at all frequencies
X-ray–TeV: correlated(?)
Radio–TeV: correlated
Optical–Radio: correlated
GeV–TeV: anticorrelated

Frail & Hjellming (1991), Casares et al. (2005), Gregory (2002)

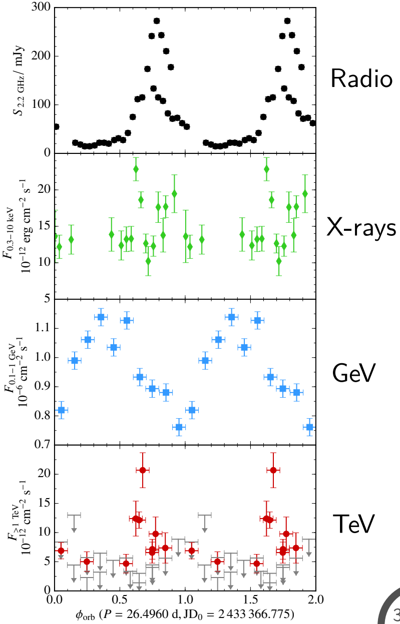

Radio emission of LS I +61 303

Large variability at radio frequencies

Emission orbitally modulated ($P_{\rm orb} \approx 26.5$ d)

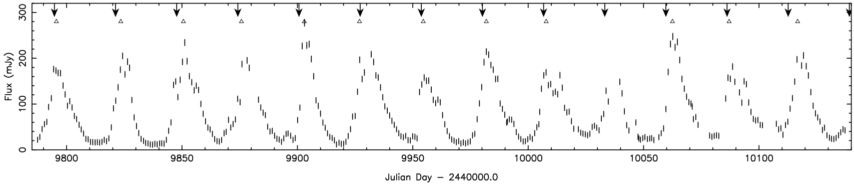

Ray et al. (1997)

The outbursts are different from cycle to cycle

Radio pulsar searches have been conducted without success
(McSwain et al. 2011, Cañellas et al. 2012)
Therefore, the observed radio emission is not pulsed

Radio emission of LS I +61 303

Focusing on a single outburst (Strickman et al. 1998)

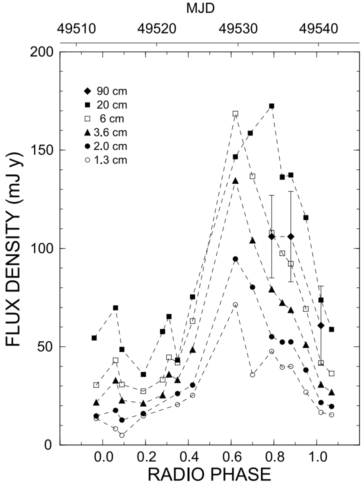

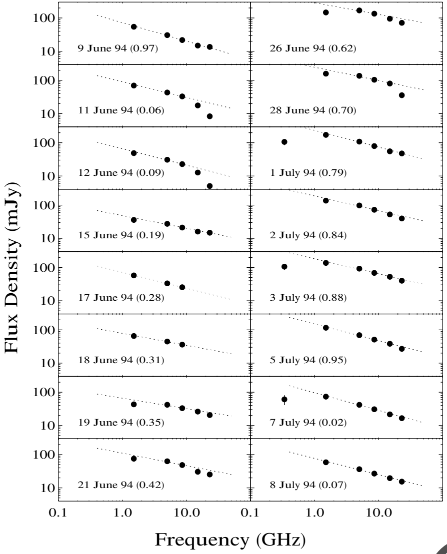

Superorbital modulation

Periodic modulation of the amplitude and the phases of these outbursts with $P_{\rm so} \approx 1\,667$ d (≈ 4.4 yr)

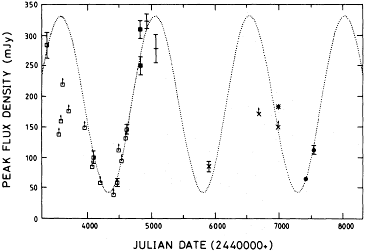

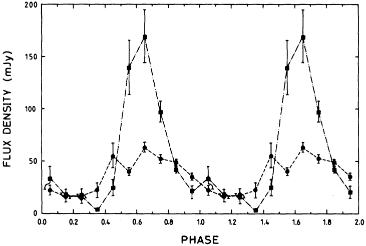

Paredes et al. (1990)

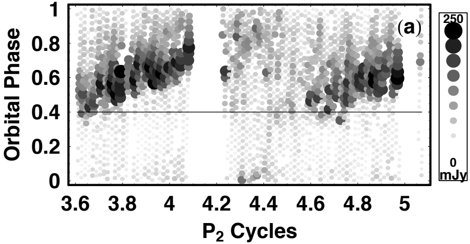

Gregory (2002)

But all these studies have been performed at GHz frequencies...!

Superorbital modulation

Periodic modulation of the amplitude and the phases of these outbursts with $P_{\rm so} \approx 1\,667$ d (≈ 4.4 yr)

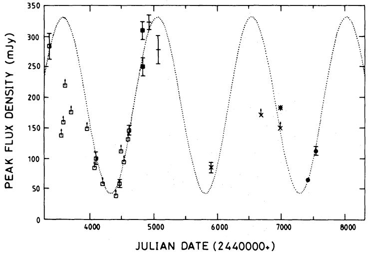

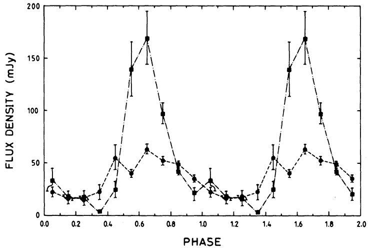

Paredes et al. (1990)

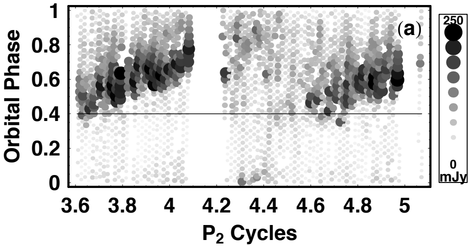

Gregory (2002)

But all these studies have been performed at GHz frequencies...!

Summary of the observations analyzed in this work

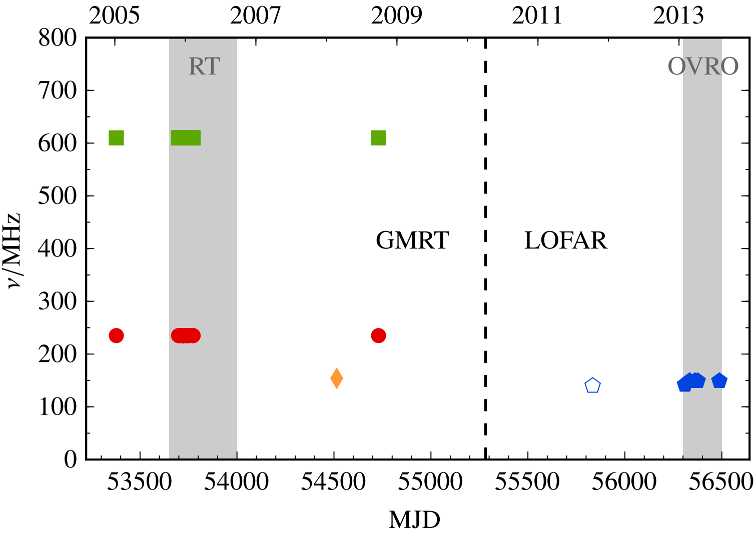

GMRT archival data analyzed in this work

LOFAR observations conducted within the TKP at our request

Radio emission of LS I +61 303

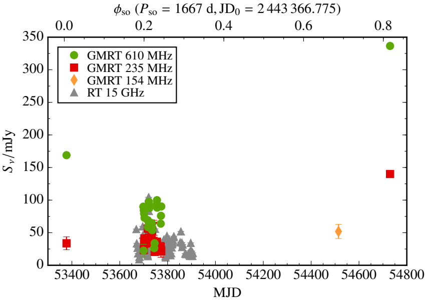

Orbital and superorbital modulation

235 MHz $\approx$ anticorrelated with 610 MHz

Significant differences between frequencies

Delays in orbital phase, $\Delta\phi$, between frequencies

Radio emission of LS I +61 303

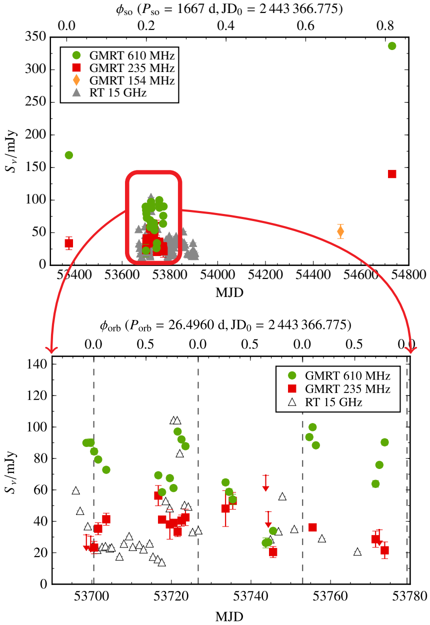

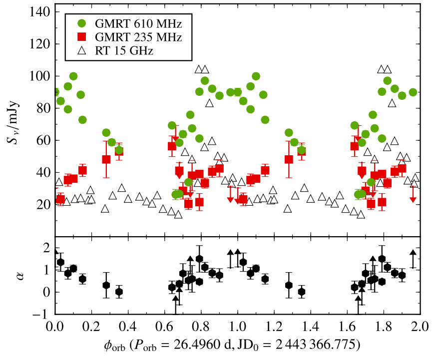

Orbital and superorbital modulation

235 MHz ≈ anticorrelated with 610 MHz

Significant differences between frequencies

Delays in orbital phase, $\Delta\phi$, between frequencies

Radio emission of LS I +61 303

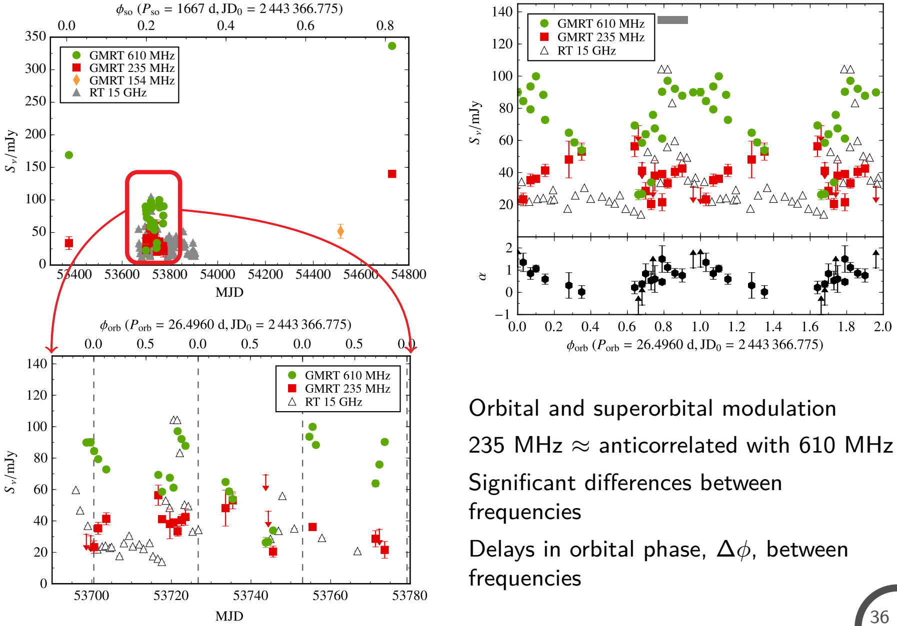

Orbital and superorbital modulation

235 MHz ≈ anticorrelated with 610 MHz

Significant differences between frequencies

Delays in orbital phase, $\Delta\phi$, between frequencies

Radio emission of LS I +61 303

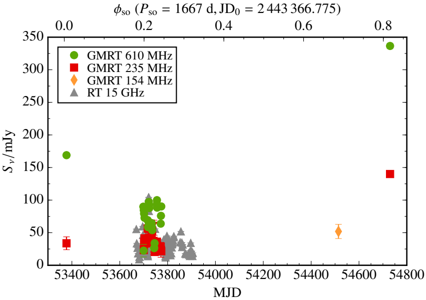

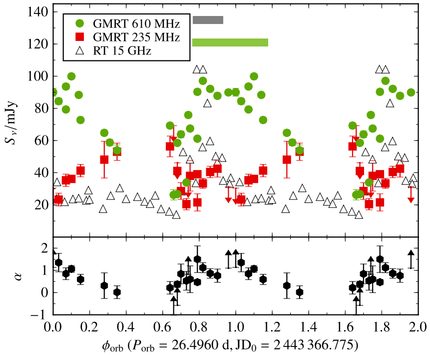

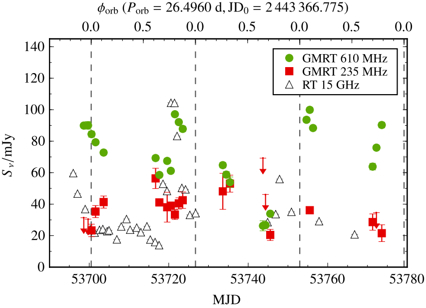

Orbital and superorbital modulation

235 MHz ≈ anticorrelated with 610 MHz

Significant differences between frequencies

Delays in orbital phase, $\Delta\phi$, between frequencies

Radio emission of LS I +61 303

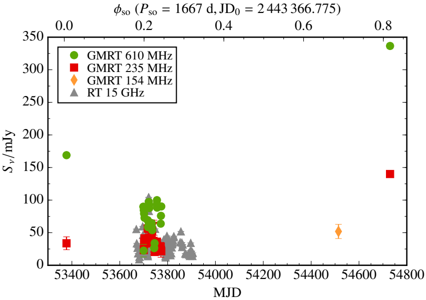

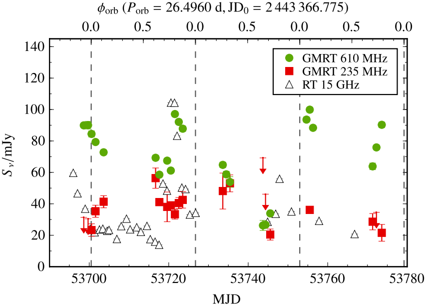

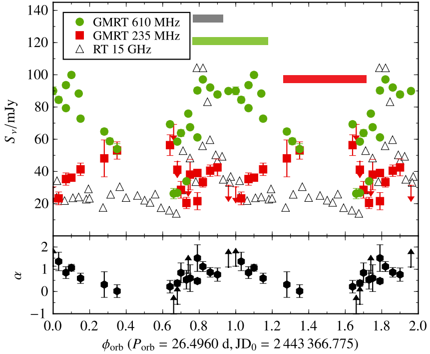

Orbital and superorbital modulation

235 MHz ≈ anticorrelated with 610 MHz

Significant differences between frequencies

Delays in orbital phase, $\Delta\phi$, between frequencies

First detection of LS I +61 303 at 150 MHz

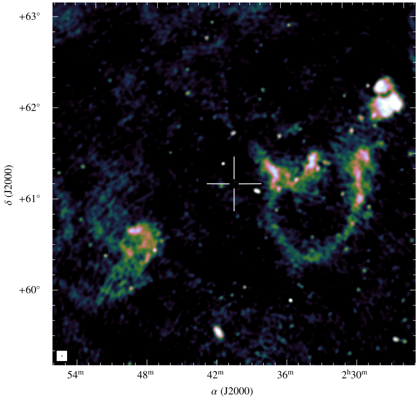

Field of view around LS I +61 303 at 150 MHz as seen by LOFAR

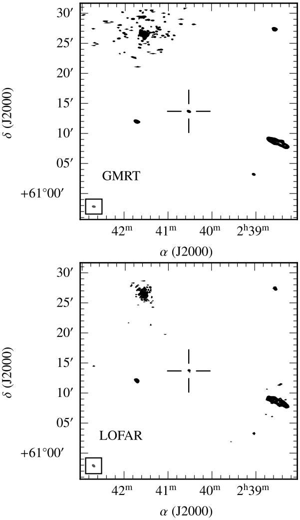

First detection of LS I +61 303 at 150 MHz

Light-curve at 150 MHz

Cannot be compared with the previous ones because of the completely different superorbital phase

Poor sampling, we can only point out a possible shift between the two frequencies, but more data is clearly needed

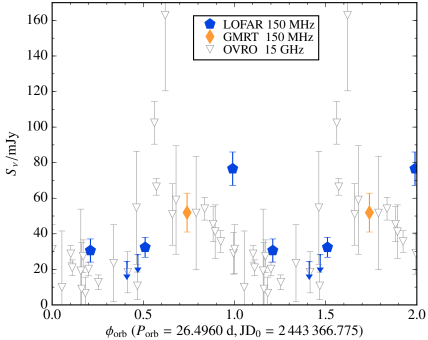

Radio emission of LS I +61 303

Light-curve at 150 MHz

Cannot be compared with the previous ones because of the completely different superorbital phase

Poor sampling, we can only point out a possible shift between the two frequencies, but more data is clearly needed

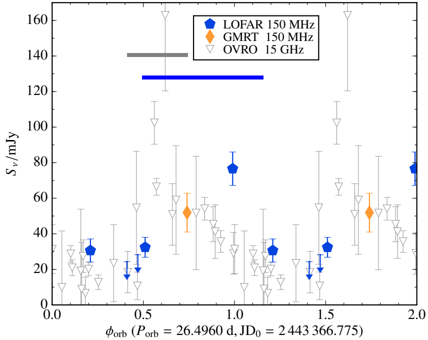

Modeling the radio emitting region

Estimating the delays between frequencies for the peak of the emission

One-zone model with an expanding radio emitting region

Delays interpreted as changes in the opacity of this region due to its expansion, considering SSA and FFA

Assuming that FFA dominates,
the expansion velocity would be

$$v_{\rm FFA} = 700 \pm 200 \ {\rm km\ s^{-1}}$$

But $\dot{M}$ is not well constrained

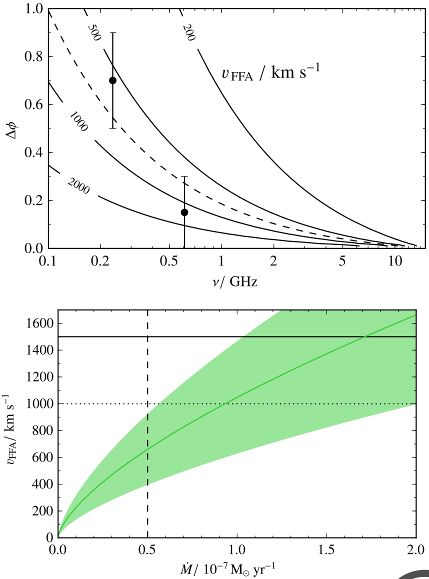

Modeling the radio emitting region

Assuming a SSA dominated region and two different dependences of B:

$\boldsymbol{B \sim \ell^{-2}}$

$$v_{\rm SSA} = 1\,000 \pm 140 \text{ km s}^{-1}$$

$\boldsymbol{B \sim \ell^{-1}}$

$$v_{\rm SSA} = 17\,000 \pm 3\,000 \text{ km s}^{-1}$$

But it is poorly constrained

FFA and SSA with $B \sim \ell^{-2}$ predict a delay of about ~ 1.0 at 150 MHz

Observed delay: 0.0–0.5 (or 1.0–1.5) but at different superorbital phase

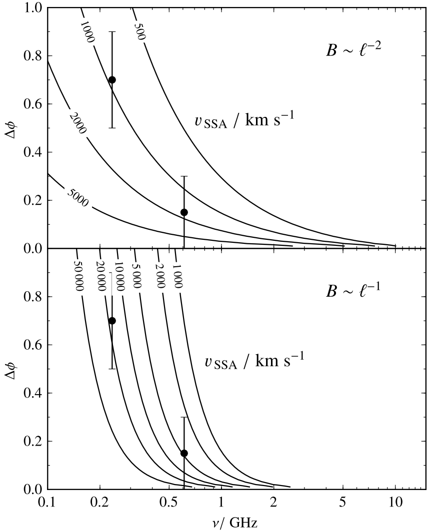

Conclusions

RESULTS

- First detection of a gamma-ray binary at a frequency as low as 150 MHz
- The superorbital variability is still present below 1 GHz
- The shape of the outbursts is significantly different at these low frequencies

DISCUSSION

- A simple model with an expanding emitting region is plausible to describe the observed behavior, leading to subrelativistic expansion velocities (that do not fit in the microquasar scenario)
- A FFA dominated or a SSA with $B \sim \ell^{-2}$ provides expansion velocities close to the stellar wind one: $\sim 1\,000$ km s^{-1}
- A SSA dominated with $B \sim \ell^{-1}$ provides a significant higher expansion velocity $\sim 17\,000$ km s^{-1}
- Although a dependence of $B \sim \ell^{-2}$ is expected in our model, it is not expected for the structure produced by the shock between the stellar and relativistic winds

Outline of the PhD Thesis

Introduction

- The γ-ray sky
- Binary systems with γ-ray emission
- Motivation of this Thesis

Part I: Gamma-ray binaries

- LS 5039 and its low-frequency emission (GMRT, VLA, WSRT)
- LS I +61 303 and its low-frequency emission (GMRT and LOFAR)
- HESS J0632+057, new EVN observations

Part II: Colliding wind binaries

- HD 93129A, a new colliding wind binary discovered

Part III: Searching for new possible gamma-ray binaries

- The candidate TYC 4051-1277-1
- MWC 656, the first Be/BH binary system

Summary and conclusions

The gamma-ray binary HESS J0632+057

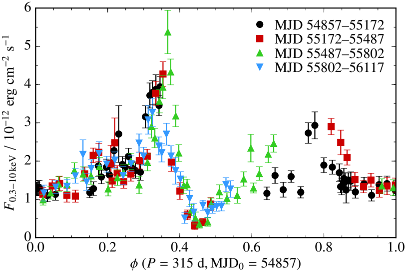

X-ray emission of HESS J0632+057 (adapted from Aliu et al. 2014)

Main X-ray outburst ($\phi \sim 0.35$)
Secondary X-ray outburst ($\phi \sim 0.6$–0.9)

X-ray–TeV correlated

Radio: only variability at VLBI scales: Extended emission filtered out

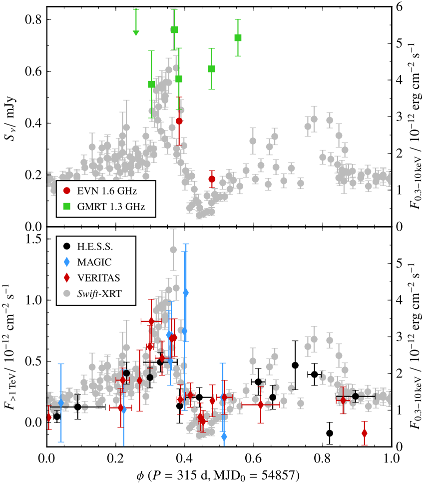

Adapted from Skilton et al. (2009), Moldón et al. (2011), Aliu et al. (2014)

EVN and WSRT observation

10-hr observation on 2014 Feb 20
$\phi = 0.76$
At 1.6 GHz

Source not detected in neither the EVN nor the WSRT data
Obtained upper-limits:

Facility	3-σ upper-limit (μJy beam^{-1})
EVN	30
WSRT	700

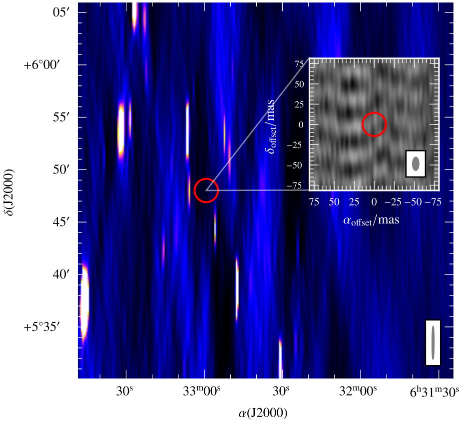

Position of HESS J0632+057 in the WSRT image and the EVN one (zoom)

Results and discussion

WSRT upper-limit at the level of previous GMRT observations

EVN upper-limit one order of magnitude fainter than previous EVN detections during the main X-ray outburst

Assuming a similar X-ray behavior at this epoch,

Epoch	$F_{\rm radio}/F_{\rm X}$
main outburst	$\sim 10^{-6}$
secondary outburst	$\lesssim 10^{-7}$

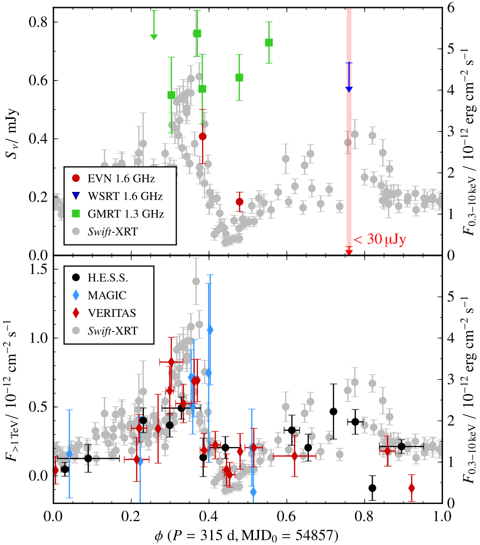

Discussion and conclusions

Why is this large decay seen during the secondary X-ray outburst?
We do not know. But, there are several possible questions/answers...

- **Do radio and X-ray emission arise from the same particle population?**
  Typically the same population of accelerated particles producing the X-ray emission also produces the radio emission
- **Non-simultaneous radio and X-ray data**
  The X-ray emission of HESS J0632+057 could be particularly faint at the epoch of the radio observations
- **Source observed before the secondary X-ray outburst took place?**
  Large differences in the profile of the secondary X-ray outburst

Outline of the PhD Thesis

Introduction
- The γ-ray sky
- Binary systems with γ-ray emission
- Motivation of this Thesis

Part I: Gamma-ray binaries
- LS 5039 and its low-frequency emission (GMRT, VLA, WSRT)
- LS I +61 303 and its low-frequency emission (GMRT and LOFAR)
- HESS J0632+057, new EVN observations

Part II: Colliding wind binaries
- HD 93129A, a new colliding wind binary discovered

Part III: Searching for new possible gamma-ray binaries
- The candidate TYC 4051-1277-1
- MWC 656, the first Be/BH binary system

Summary and conclusions

The colliding wind binary HD 93129A

HD 93129A

O2 If* star (Aa)
O3.5 V star (Ab)
$d \sim 2.5$ kpc at the Carina nebula

System mass: $200 \pm 45\ \mathrm{M}_\odot$
$v_\infty = 3200 \pm 200$ km s^{-1}
System luminosity: $\sim 1.6 \times 10^6\ \mathrm{L}_\odot$
X-ray luminosity: $\sim 1.3 \times 10^{-7}\ \mathrm{L}_{\rm bol}$
Non-thermal radio emission coincident with the system: 1–10 mJy at 1.4–24.5 GHz

Walborn (1995), Taresch et al. (1997), Walborn et al. (2002), Repolust et al. (2004), Benaglia et al. (2006), Maíz Apellániz et al. (2008)

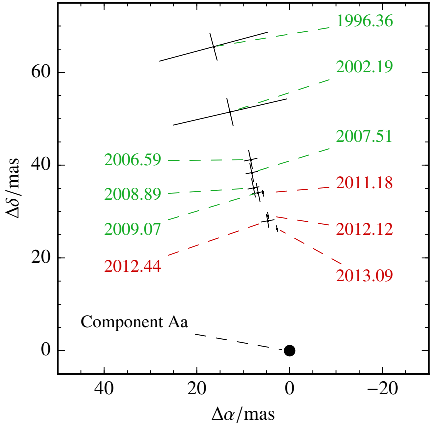

Motivation and multiwavelength campaign

The two massive stars could form a binary system
A close distance between them would produce a wind collision region

Multiwavelength campaign to unveil the nature of this system:

- **Optical**
  HST observations: accurate astrometry of both components and their relative proper motions
- **Radio**
  LBA observation: to resolve the radio emission and its location
  ATCA observations: determination of the radio spectrum

The multiwavelength data would clarify the possible nature of this system and if HD 93129A is a colliding wind binary

Radio observations

We have analyzed an observation conducted on 2008 August 6 at 2.3 GHz with five LBA antennas (Parkes, Mopra, ATCA, Ceduna and Hobart)

The synthesized beam is 15×11 mas^2, PA$= 85^\circ$

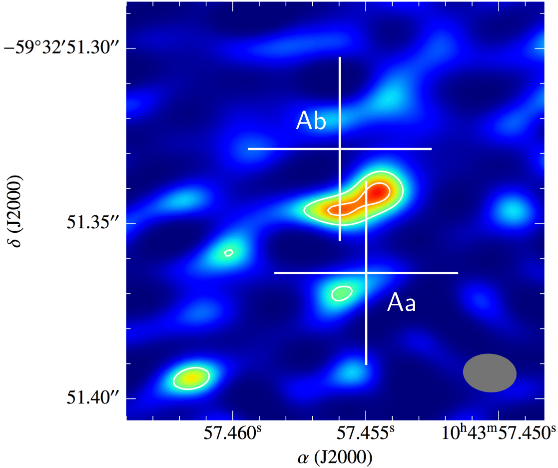

The relative separation of the stars is 36 ± 1 mas and PA$= 12 \pm 1^\circ$

Results and discussion

Estimating the wind-momentum rates

Ratio between the wind momentum rates of the two stars:

$$\eta = \left(\frac{R_\mathrm{b}}{R_\mathrm{a}}\right)^2 = \frac{\dot{M}_\mathrm{b} v_\mathrm{b}}{\dot{M}_\mathrm{a} v_\mathrm{a}}$$

Assuming the position of the two stars (inferred from the *HST*/FGS data),

$$\eta \sim 0.5$$

Distance between stars enough to reach the terminal wind velocity values, $v_\mathrm{b} \sim v_\mathrm{a}$, and then

$$\dot{M}_\mathrm{b} \sim 0.5 \dot{M}_\mathrm{a}$$

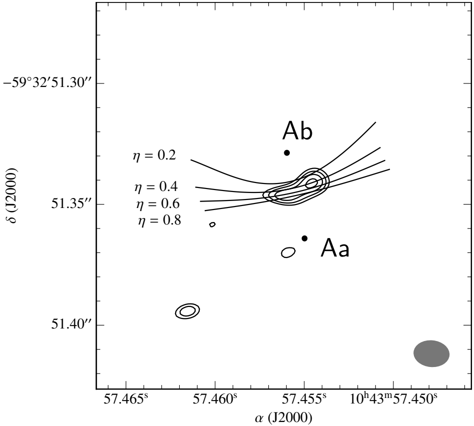

Results and discussion

ATCA data from observations conducted in 2003–2009 at 1.4–24 GHz

Spectral indexes (unabsorbed region):

$\alpha = -1.03 \pm 0.09$
$\alpha = -1.21 \pm 0.03$

Stronger emission from 2003 to 2009 ($\sim$ 40% increase)

Drift of the turnover frequency, indicative of a stronger and denser WCR

Both expected if approaching to periastron

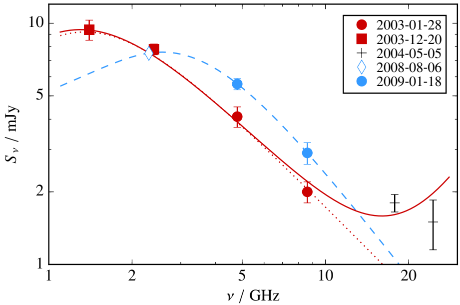

Synchrotron emission models plus FFA and thermal component

Discussion and conclusions

- **A new colliding wind binary**
  The presence of an extended and curved radio emission coincident with a position between the two stars and orthogonal to the line joining them is the best argument to consider HD 93129A as a new colliding wind binary
- **Wind-momentum rates**
  Rough estimation of the wind-momentum rates ratio, $\eta \sim 0.5$
- **Estimation of the orbital parameters**
  No accurate estimation of the putative orbit. Our fit suggests:
  $P_{\rm orb} \sim 200$ yr, $e \gtrsim 0.9$, and the periastron passage in 2024
- **In the future...**
  We expect an enhanced radio emission during the approach to periastron. If the distance is small enough, HD 93129A could even show γ-ray emission

Outline of the PhD Thesis

Introduction

- The γ-ray sky
- Binary systems with γ-ray emission
- Motivation of this Thesis

Part I: Gamma-ray binaries

- LS 5039 and its low-frequency emission (GMRT, VLA, WSRT)
- LS I +61 303 and its low-frequency emission (GMRT and LOFAR)
- HESS J0632+057, new EVN observations

Part II: Colliding wind binaries

- HD 93129A, a new colliding wind binary discovered

Part III: Searching for new possible gamma-ray binaries

- The candidate TYC 4051-1277-1
- MWC 656, the first Be/BH binary system

Summary and conclusions

The candidate TYC 4051-1277-1

Cross-identification between the optical LS catalog and the WENSS/NVSS radio surveys

B9 star coincident with a NT radio source

WSRT and VLA observations conducted to verify this possible association

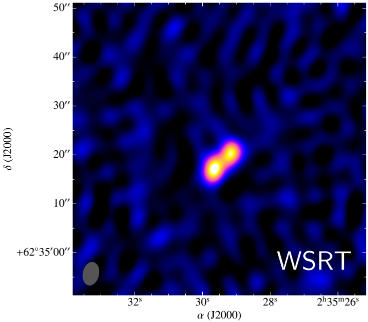

Blended double-lobed shape
Spectrum clearly non-thermal
Typical from a radio galaxy

The astrometry rejects the possible association

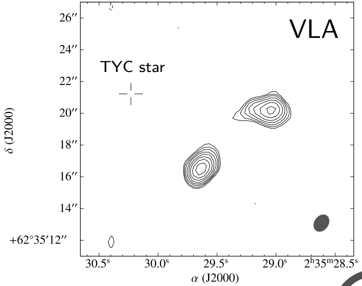

We unveiled the nature of this radio source and rejected its association with the B9 star
Compatible with an unassociated *Fermi* source

MWC 656, the first Be/BH binary system

Introduction

- γ-ray flare detected by *AGILE* on 2012 above 100 MeV (Lucarelli et al. 2010)
- Two possible origins: the quasar RX J2243.1+4441 and the Be star MWC 656 (Williams et al. 2010)
- Photometric period of 60.37 ± 0.04 d
- Casares et al. (2014) reported the presence of a black hole of 3.8–6.9 $\mathrm{M}_{\odot}$
- Multiwavelength campaign to study in detail the source from radio to TeV

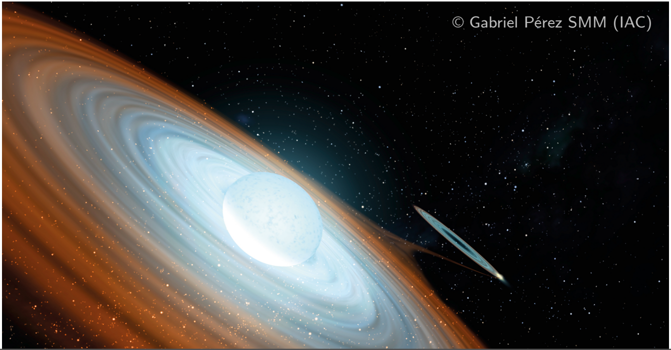

MWC 656, the first Be/BH binary system

Searching for the radio counterpart

Five WSRT observations at 1.4 GHz

Strong quasar affecting the FoV

Three VLA observations at 3.0 GHz

We do not detect MWC 656

Most restrictive 3-σ upper-limit: 40 µJy beam^{-1}

Better coverage of the orbit

About the quasar:

Persistent compact core of ~ 2 mJy

Variability in the south lobe, increase of a factor 2 in 10 d

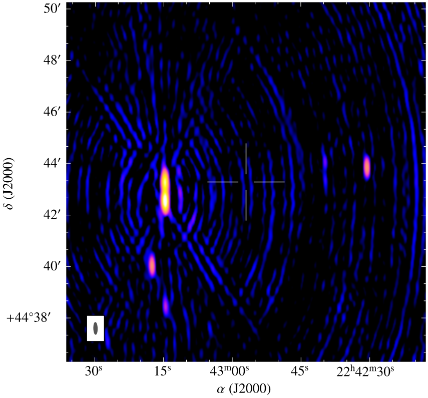

MWC 656, the first Be/BH binary system

Searching for the radio counterpart

Five WSRT observations at 1.4 GHz

Strong quasar affecting the FoV

Three VLA observations at 3.0 GHz

We do not detect MWC 656

Most restrictive 3-σ upper-limit: 40 μJy beam^{-1}

Better coverage of the orbit

About the quasar:

Persistent compact core of $\sim$ 2 mJy

Variability in the south lobe, increase of a factor 2 in 10 d

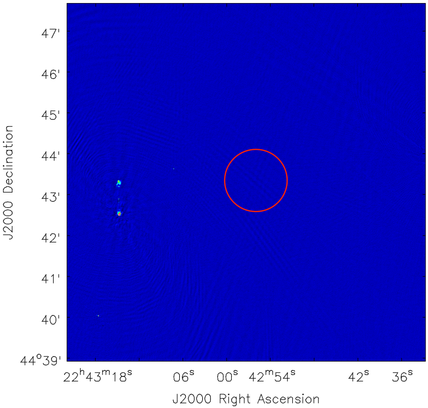

MWC 656, the first Be/BH binary system

Searching for the radio counterpart

Five WSRT observations at 1.4 GHz

Strong quasar affecting the FoV

Three VLA observations at 3.0 GHz

We do not detect MWC 656

Most restrictive 3-σ upper-limit: 40 μJy beam^{-1}

Better coverage of the orbit

About the quasar:

Persistent compact core of $\sim$ 2 mJy

Variability in the south lobe, increase of a factor 2 in 10 d

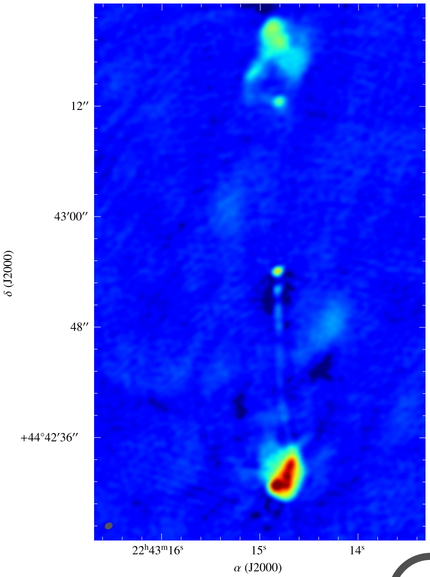

MWC 656, the first Be/BH binary system

Conclusions

- MWC 656 remains undetected at radio frequencies.
  The radio to X-ray correlation observed in BH HMXBs predicts a flux density just below the current upper-limits

- The current radio observations cover different orbital phases, and we discard radio emission above $\sim 50\ \mu$Jy

- The quasar is still a possible candidate to produce γ-ray flares. However, the core seems to be quite stable along the time

- The fast variability observed in the south lobe must be studied in detail

Outline of the PhD Thesis

Introduction

- The γ-ray sky
- Binary systems with γ-ray emission
- Motivation of this Thesis

Part I: Gamma-ray binaries

- LS 5039 and its low-frequency emission (GMRT, VLA, WSRT)
- LS I +61 303 and its low-frequency emission (GMRT and LOFAR)
- HESS J0632+057, new EVN observations

Part II: Colliding wind binaries

- HD 93129A, a new colliding wind binary discovered

Part III: Searching for new possible gamma-ray binaries

- The candidate TYC 4051-1277-1
- MWC 656, the first Be/BH binary system

Summary and conclusions

Summary of observations presented in the Thesis

Source	Facility	Freqs. (GHz)	Year	Type	Comments
LS 5039	VLA	1–15	'98,02	A	First detailed study at low-freq. (Razin effect)
	WSRT	1–5	'13	PI	
	GMRT	0.15–0.61	'04–08,13	A/PI	
LS I +61 303	GMRT	0.15–0.61	'05–08	A	Discovery of orbital variability at low-freq. and first detection at 150 MHz
	LOFAR	0.15	'13	C	
HESS J0632+057	EVN	1.6	'14	PI	First VLBI observation during secondary X-ray outburst
HD 93129A	LBA	2.3	'08	A	Discovery of the CWB
TYC 4051-1277-1	WSRT	2.3	'12	PI	First search
MWC 656	WSRT	1.4	'11–12	PI	First search with connected interferometers
	VLA	3.0	'12	PI	Deep images. Study of quasar

A: **archival data analyzed by the author**
PI: **observations conducted and analyzed by the author as PI**
C: **observations conducted as co-I and analyzed by the author**

Conclusions of the Thesis (1/2)

LS 5039

- Persistent variability from day to year timescales with a small variability from low to high frequencies
- Clarification of the previously contradictory results at low frequencies
- Determination of the presence of a persistent turnover at ~ 0.5 GHz
- Explanation of the spectra with a simple model considering different absorption processes. First time that the Razin effect is observed in a gamma-ray binary

LS I +61 303

- First detection at 150 MHz with GMRT and LOFAR
- Detection of the superorbital modulation at low frequencies
- Study of the orbital variability at low frequencies, reporting significant differences as a function of the frequency
- An expanding emitting region can explain the observed delays between the peak of the maximum emission, with a clearly subrelativistic expansion velocity. For some models the expansion velocity is close to the stellar wind one

Low frequency radio observations have proven to be an important tool to explore physical parameters of the emitting regions in gamma-ray binaries

Conclusions of the Thesis (1/2)

LS 5039

- Persistent variability from day to year timescales with a small variability from low to high frequencies
- Clarification of the previously contradictory results at low frequencies
- Determination of the presence of a persistent turnover at ~ 0.5 GHz
- Explanation of the spectra with a simple model considering different absorption processes. First time that the Razin effect is observed in a gamma-ray binary

LS I +61 303

- First detection at 150 MHz with GMRT and LOFAR
- Detection of the superorbital modulation at low frequencies
- Study of the orbital variability at low frequencies, reporting significant differences as a function of the frequency
- An expanding emitting region can explain the observed delays between the peak of the maximum emission, with a clearly subrelativistic expansion velocity. For some models the expansion velocity is close to the stellar wind one

Low frequency radio observations have proven to be an important tool to explore physical parameters of the emitting regions in gamma-ray binaries

Conclusions of the Thesis (2/2)

HESS J0632+057

- First VLBI observations during the secondary X-ray outburst
- Strong decay of at least one order of magnitude of its radio emission, which is not seen at other wavelengths

HD 93129A

- Discovery of this new colliding wind binary with multiwavelength observations
- Rough estimation of the wind-momentum rates ratio with the study of the wind collision region

TYC 4051-1277-1

- No radio counterpart found
- Identification of a field radio source as a radio galaxy

MWC 656

- Upper-limits for the radio emission at different orbital phases
- First measurements of the radio flux density for different parts of the quasar RX J2243.1+4441

Thank you!

Back-up slides

Introduction

The gamma-ray sky

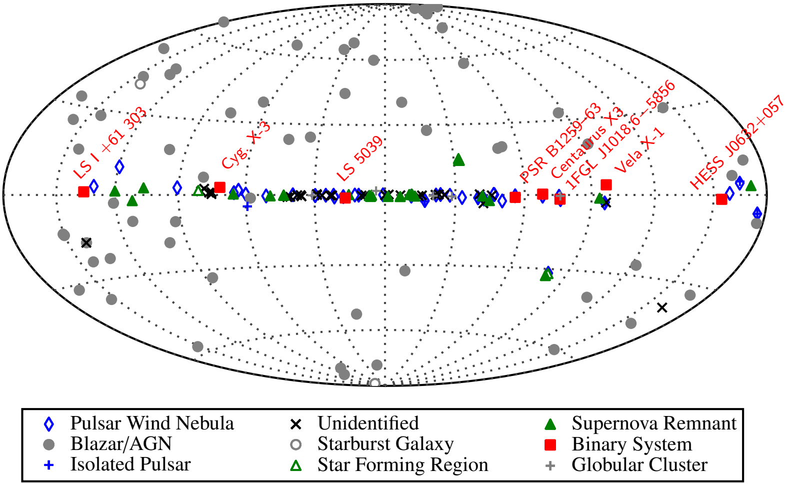

Very high-energy γ-ray all-sky map showing the 161 sources discovered up to now emitting at TeV energies. TevCat catalog (`tevcat.uchicago.edu`).

Accurate GMRT data reduction (Marcote et al. 2015, Appendix)

We are observing radio sources within the Galactic Plane, but using flux calibrators outside the G. Plane

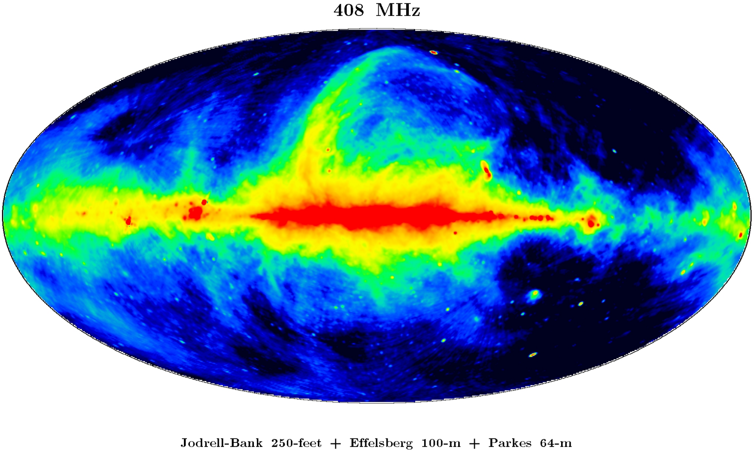

Accurate GMRT data reduction (Marcote et al. 2015, Appendix)

We are observing radio sources within the Galactic Plane, but using flux calibrators outside the G. Plane

- The Galactic diffuse emission contributes differently to the target source than to the flux calibrators, affecting to the $T_{\rm sys}$ of the antennas
- The $T_{\rm sys}$ needs to be compensated to properly estimate the flux density values in the target field of view
- Usually done automatically in most telescopes. Not in the case of GMRT
- Godambe et al. (2008) did not take into account these corrections
- Pandey et al. (2007) used the *Haslam approximation*
- We conducted dedicated non-correlated observations with the GMRT to directly measure the Galactic contribution to properly subtract it
- We observed significant differences between these two methods (as noted in Sirothia 2009)

Razin effect

The synchrotron emission propagates through a plasma, which presents a refractive index n. Always that $n < 1$ the beaming effect is partially suppressed. Although at high frequencies the effect is negligible, at low frequencies (with $\nu \ll \nu_\mathrm{p}$, where ν_p is the plasma frequency) it suppresses the beaming effect since

$$n^2 = 1 - \left(\frac{\nu_\mathrm{p}}{\nu}\right)^2$$

and the beaming effect goes as

$$\theta_\mathrm{b} \approx \gamma^{-1} = \sqrt{1 - n^2\beta^2}$$

- Presence of a thermal plasma surrounding the emitting region.
- Attenuation of the synchrotron radiation at low frequencies.
- Widely reported in Colliding Wind Binaries, solar wind,...
- A good approximation is an exponential attenuation at low frequencies (Dougherty et al. 2003):

$$S_\nu \propto S_\nu e^{-\nu_\mathrm{R}/\nu}, \qquad \nu_\mathrm{R} \equiv 20 n_\mathrm{e} B^{-1}$$

WSRT observations of TYC 4051-1277-1

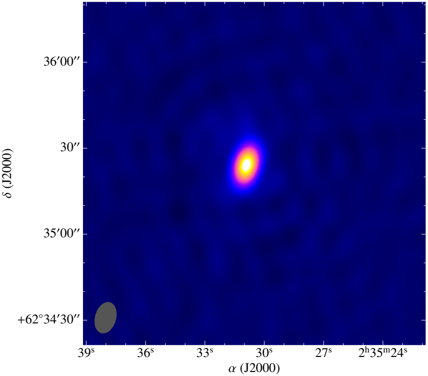

2.3 GHz data
Point-like source
6.23 ± 0.13 mJy

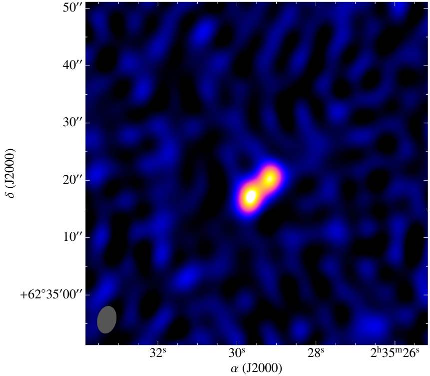

4.9 GHz data
Double-lobed structure
3.19 ± 0.09 mJy

$\alpha \approx -0.88 \pm 0.17$

List of publications

- **Marcote, B.**, et al., 2015, MNRAS, submitted
- **Marcote, B.**, Ribó, M., Paredes, J. M., Ishwara-Chandra, C. H., 2015, MNRAS, 451, 4578
- Benaglia, P., **Marcote, B.**, Moldón, J., Nelan, E., De Becker, M., Dougherty, S. M., Koribalski, B., 2015, A&A, 579, A99
- Martí, J., Luque-Escamilla, P L., Casares, J., **Marcote, B.**, Paredes-Fortuny, X., Ribó, M., Paredes, J. M., Núñez, J., 2015, Ap&SS, 356, 277
- **Marcote, B.**, Benaglia, P., Moldón, J., Nelan, E., De Becker, M., Dougherty, S. M., Koribalski, B., 2014, in proceedings of the 12th European VLBI Network Symposium and Users Meeting. Cagliari, Italy, PoS(EVN2014)57
- **Marcote, B.**, Moldón, J., Ribó, M., Paredes, J. M., Paragi, Z., 2014, in proceedings of the 12th European VLBI Network Symposium and Users Meeting. Cagliari, Italy, PoS(EVN2014)95
- **Marcote, B.**, Ribó, M., Paredes, J. M., Ishwara-Chandra, C. H., Swinbank, J., Broderick, J., Fender, R., Markoff, S., Wijers, R., 2014, in proceedings of The Metrewavelength Sky Conference. Pune, India, Bull. Astr. Soc. India
- **Marcote, B.**, Ribó, M., Paredes, J. M., Swinbank, J., Broderick, J., Fender, R., Markoff, S., Wijers, R., 2012, AIP Conf. Proc., 1505, 374

Future work (open projects)

- We have been granted with low-frequency GMRT observations covering a full orbital cycle of LS I +61 303 (and we expect the decision for simultaneous LOFAR ones)
- We will propose observations of HD 93129A with the LBA during the coming years
- MWC 656 has recently been observed deeply with *Chandra* and the VLA (data analysis ongoing)
- HESS J0632+057 could be re-observed several times with the EVN, ideally with simultaneous X-ray observations